An Investigation of 1:1 Adducts of Gallium Trihalides with Triarylphosphines by Solid-State 69/71Ga and 31PNMR Spectroscopy

ARTICLE *in* CHEMISTRY · FEBRUARY 2013

Impact Factor: 5.73 · DOI: 10.1002/chem.201202954 · Source: PubMed

7 AUTHORS, INCLUDING:

Fu Chen
University of Iowa
14 PUBLICATIONS **147** CITATIONS
SEE PROFILE

Guibin Ma
KTH Royal Institute of Technology
36 PUBLICATIONS **452** CITATIONS
SEE PROFILE

Roderick E. Wasylishen
University of Alberta
401 PUBLICATIONS **6,539** CITATIONS
SEE PROFILE

CHEMISTRY
A EUROPEAN JOURNAL

ChemPubSoc
Europe

DOI: 10.1002/chem.201202954

An Investigation of 1:1 Adducts of Gallium Trihalides with Triarylphosphines by Solid-State $^{69/71}$Ga and ^{31}P NMR Spectroscopy

Fu Chen, Guibin Ma, Guy M. Bernard, Roderick E. Wasylishen,* Ronald G. Cavell, Robert McDonald, and Michael J. Ferguson[a]

Abstract: Several 1:1 adducts of gallium trihalides with triarylphosphines, $X_3Ga(PR_3)$ (X = Cl, Br, and I; PR_3 = triarylphosphine ligand), were investigated by using solid-state $^{69/71}$Ga and ^{31}P NMR spectroscopy at different magnetic-field strengths. The $^{69/71}$Ga nuclear quadrupolar coupling parameters, as well as the gallium and phosphorus magnetic shielding tensors, were determined. The magnitude of the ^{71}Ga quadrupolar coupling constants ($C_Q(^{71}Ga)$) range from approximately 0.9 to 11.0 MHz. The spans of the gallium magnetic shielding tensors for these complexes, $\delta_{11}-\delta_{33}$, range from approximately 30 to 380 ppm; those determined for phosphorus range from 10 to 40 ppm. For any given phosphine ligand, the gallium nuclei are most shielded for X = I and least shielded for X = Cl, a trend previously observed for In^{III}–phosphine complexes. This experimental trend, attributed to spin-orbit effects of the halogen ligands, is reproduced by DFT calculations. The signs of $C_Q(^{69/71}Ga)$ for some of the adducts were determined from the analysis of the ^{31}P NMR spectra acquired with magic angle spinning (MAS). The $^1J(^{69/71}Ga,^{31}P)$ and $\Delta J(^{69/71}Ga,^{31}P)$ values, as well as their signs, were also determined; values of $^1J(^{71}Ga,^{31}P)$ range from approximately 380 to 1590 Hz. Values of $^1J(^{69/71}Ga,^{31}P)$ and $\Delta J(^{69/71}Ga,^{31}P)$ calculated by using DFT have comparable magnitudes and generally reproduce experimental trends. Both the Fermi-contact and spin-dipolar Fermi-contact mechanisms make important contributions to the $^1J(^{69/71}Ga,^{31}P)$ tensors. The ^{31}P NMR spectra of several adducts in solution, obtained as a function of temperature, are contrasted with those obtained in the solid state. Finally, to complement the analysis of NMR spectra for these adducts, single-crystal X-ray diffraction data for $Br_3Ga[P(p\text{-Anis})_3]$ and $I_3Ga[P(p\text{-Anis})_3]$ were obtained.

Keywords: chemical shifts · coupling constants · density functional calculations · gallium · NMR spectroscopy · phosphorus

Introduction

Interest in the study of adducts formed by Group 13 Lewis acids with Group 15 Lewis bases dates back to the early 1800s with the first synthesis of $F_3B{\cdot}NH_3$ by Gay-Lussac and Thénard.[1] The preparation of adducts formed by the Group 13 (B, Al, Ga, In, Tl) trihalides or trialkyls with Lewis bases containing Group 15 elements (N, P, As, Sb, Bi) has drawn considerable recent attention[2] because they have many important applications, particularly in materials chemistry.[3,4,5] For example, they are single-source precursors for preparing a wide range of semiconductors based on Group 13 and 15 elements.[3] In the case of gallium, GaN and GaP are used extensively in light-emitting diodes (LEDs),[5] GaSb is used in thermal-imagining devices[5] and GaAs is widely used in solar cells.[5] The gallium trihalide phosphine adducts were first prepared and characterized by Carty and co-workers,[6] and have remained of interest because of their importance in the preparation of GaP-based semiconductors.[7]

Gallium trihalide phosphine adducts have often been characterized by using single-crystal X-ray diffraction or vibrational spectroscopy.[6,8–10] Herein, we show that solid-state $^{69/71}$Ga and ^{31}P NMR spectroscopy are excellent complementary techniques for characterizing 1:1 adducts of gallium trihalides with triarylphosphines. The information available from NMR spectroscopy includes the chemical shift (CS) tensors, indirect spin–spin coupling constants between $^{69/71}$Ga and ^{31}P, and the electric field gradient (EFG) tensors for the quadrupolar nuclei, ^{69}Ga and ^{71}Ga. Previously, solid-state $^{69/71}$Ga NMR spectroscopy has been used to determine the nuclear quadrupolar coupling constants ($C_Q(^{69/71}Ga)$) for Ga_2O_3[11] and various semiconductors, including

[a] Dr. F. Chen, Dr. G. Ma, Dr. G. M. Bernard, Prof. R. E. Wasylishen, Prof. R. G. Cavell, Dr. R. McDonald, Dr. M. J. Ferguson
Department of Chemistry, University of Alberta
Edmonton, Alberta, T6G 2G2 (Canada)
Fax: (+1) 780-492-8231
E-mail: Roderick.Wasylishen@ualberta.ca

Supporting information for this article is available on the WWW under http://dx.doi.org/10.1002/chem.201202954. It contains background information on nuclear quadrupole coupling, magnetic shielding, and indirect spin–spin coupling; sample preparation; quantum chemical calculations; single-crystal X-ray diffraction data for $Br_3Ga[P(p\text{-Anis})_3]$ and $I_3Ga[P(p\text{-Anis})_3]$; a summary of 2*d* values; computational gallium magnetic shielding parameters; additional solid-state ^{31}P and $^{69/71}$Ga NMR spectra for all adducts at different magnetic-field strengths; and solution-phase ^{31}P NMR spectra for all adducts at different temperatures.

GaN,[12] GaP,[13] and GaAs;[14] nevertheless, the study of gallium complexes by using solid-state $^{69/71}$Ga NMR spectroscopy is limited.[15] Gallium isotropic chemical shifts (δ_{iso}(Ga)) range over approximately 1400 ppm;[16] therefore, one might expect gallium chemical shift anisotropy (CSA) to be large. However, there have only been a few reports of gallium CSAs.[11a,17]

Previously, we undertook a detailed solid-state NMR investigation of some related indium trihalide phosphine adducts.[18,19] In those studies, we showed that a careful analysis of ^{115}In and ^{31}P NMR spectra could provide considerable information about these adducts. Hence, a goal of this study is to determine whether the similarity of the gallium trihalide triarylphosphines with the 1:1 indium–phosphine adducts investigated in the earlier studies will be reflected in their NMR properties. Specifically, 1:1 adducts of gallium trihalide with a triarylphosphine, $X_3Ga(PR_3)$ (X = Cl, Br, and I; PR_3 = triarylphosphine ligand), are characterized by using solid-state $^{69/71}$Ga and ^{31}P NMR spectroscopy; these NMR results are corroborated by the results of density functional theory (DFT) calculations. Possible causes for the observed sensitivity of the gallium CS tensors to the nature of the halogen ligands are considered. In addition, analyses of the ^{31}P NMR spectra allowed the determination of $^1J(^{69/71}Ga,^{31}P)$ and $\Delta J(^{69/71}Ga,^{31}P)$, that is, the anisotropy in $^1J(^{69/71}Ga,^{31}P)$. The signs for $\Delta J(^{69/71}Ga,^{31}P)$, $^1J(^{69/71}Ga,^{31}P)$, and $C_Q(^{69/71}Ga)$ were also determined for these adducts. In addition, since knowledge of the structures of the adducts under study is invaluable for a proper analysis of the $^{69/71}$Ga and ^{31}P NMR spectra, single-crystal X-ray diffraction data for $Br_3Ga[P(p\text{-Anis})_3]$ and $I_3Ga[P(p\text{-Anis})_3]$ (Anis = anisole, $C_6H_4(OCH_3)$) are also presented.

Gallium NMR spectroscopy: Gallium has two naturally occurring isotopes: ^{69}Ga and ^{71}Ga. The nuclear-spin properties and natural abundance (NA) of the two isotopes, ^{69}Ga ($S = {}^3/_2$, $\Xi = 24.00\,\%$, $Q = 17.1$ fm^2, NA = 60.1 %) and ^{71}Ga ($S = {}^3/_2$, $\Xi = 30.50\,\%$, $Q = 10.7$ fm^2, NA = 39.9 %),[20] make them potential candidates for NMR spectroscopic study. In the solid state, ^{71}Ga is the preferred gallium NMR isotope because of its larger Larmor frequency and receptivity, as well as its smaller nuclear quadrupolar moment. Nevertheless, in many studies, including this work, both ^{69}Ga and ^{71}Ga are investigated. In an applied magnetic field, $\mathbf{B}_0$, the interactions involving the $^{69/71}$Ga nuclei of $X_3Ga(PR_3)$ include the Zeeman, nuclear quadrupolar, and nuclear magnetic shielding interactions, as well as the direct dipolar and indirect nuclear spin–spin coupling interactions between $^{69/71}$Ga and coupled ^{31}P nuclei ($I = {}^1/_2$, NA = 100 %).

NMR spectroscopists typically measure chemical shifts, δ, the nuclear magnetic shielding of a given nucleus relative to that for a reference compound: $\delta \approx \sigma_{ref} - \sigma_{sample}$, in which the latter two terms refer to the magnetic shielding of the reference compound and of the sample, respectively.[21] When discussing NMR spectra, it is convenient to use three chemical shift parameters: the isotropic chemical shift, $\delta_{iso} = (\delta_{11} + \delta_{22} + \delta_{33})/3$, in which $\delta_{11} \geq \delta_{22} \geq \delta_{33}$, the span, $\Omega = \delta_{11} - \delta_{33}$, describing the maximum orientation dependence of the magnetic shielding interaction, and the skew, $\kappa = 3(\delta_{22} - \delta_{iso})/\Omega$, which is unitless with $-1 \leq \kappa \leq +1$;[21] note that for an axially symmetric chemical shift tensor, $\kappa = \pm 1$.

The effects of the nuclear quadrupolar coupling interaction on solid-state NMR spectra of quadrupolar and spin-$^1/_2$ nuclei have been discussed extensively;[22] a summary is also presented in the Supporting Information. Likewise, readers are encouraged to consult the original literature[22d,23,24] or Supporting Information for a detailed discussion of the effects of direct and indirect spin–spin interactions on NMR spectra.

^{31}P NMR spectroscopy of the $^{69/71}$Ga–^{31}P spin pair: A ^{31}P NMR spectrum spin–spin coupled to either ^{69}Ga or ^{71}Ga should consist of four peaks (Figure 1).[25] If C_Q is significant, the direct dipolar interaction for the $^{69/71}$Ga–^{31}P spin pair is not averaged to zero by magic angle spinning (MAS),[25] a consequence of the fact that the gallium nuclei are not quantized exactly along $\mathbf{B}_0$.[26] In this case, one observes an uneven spacing between adjacent peaks (Figure 1); analysis of these spectra yield the residual dipolar coupling (d), which is directly related to C_Q and R_{eff}. In favorable cases, such analyses will also yield the sign of C_Q; see the Supporting Information for a presentation of the underlying theory.

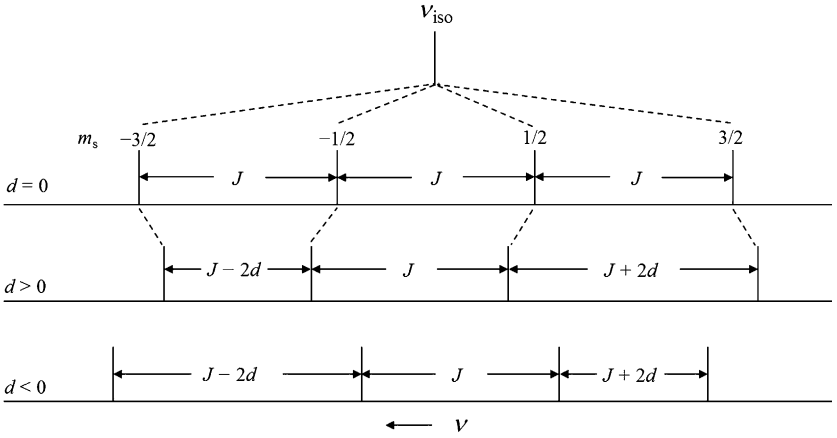

Figure 1. Calculated splitting pattern in a ^{31}P NMR spectrum of a MAS sample containing a $^{69/71}$Ga–^{31}P spin pair with $d = 0$, $d > 0$, and $d < 0$. The spin states as indicated are those for a positive sign for $^1J(^{69/71}Ga,^{31}P)$, but the splitting pattern is invariant with this sign.

Results and Discussion

Because of the importance of molecular structure in the analysis of the NMR results, those for the triarylphosphine gallium trihalide adducts are presented first, followed by a discussion of the solid-state $^{69/71}$Ga NMR spectra of each adduct. Next, the $^{1}J(^{69/71}\mathrm{Ga},^{31}\mathrm{P})$ and $\Delta J(^{69/71}\mathrm{Ga},^{31}\mathrm{P})$ values, as well as their signs, and the $C_{\mathrm{Q}}(^{69/71}\mathrm{Ga})$ values for all complexes, determined through ^{31}P NMR spectroscopy, are reported. Finally, results of relativistic DFT calculations of the NMR parameters for these compounds are compared with experimental values and the causes of the observed sensitivity of the gallium CS tensors to the nature of the directly bonded halogen ligands are explored.

Structures of the triarylphosphine gallium trihalide adducts: Structures for $Cl_3Ga(PPh_3)$,[8] $Br_3Ga(PPh_3)$,[8] and $I_3Ga(PPh_3)$,[9] obtained from X-ray crystallography, have been reported; those for $Br_3Ga[P(p\text{-Anis})_3]$ and $I_3Ga[P(p\text{-Anis})_3]$ were determined as part of this study and are shown in Figure 2. See Tables S1 and S2 in the Supporting Information for more detailed X-ray diffraction data and for selected structural information. All five adducts studied by X-ray crystallography have approximately tetrahedral coordination about the Ga and P atoms; there is a C_3 axis along the Ga–P bond of $I_3Ga(PPh_3)$ and $Br_3Ga[P(p\text{-Anis})_3]$ and an approximate C_3 axis along this bond for the other adducts.

We were unable to obtain crystals suitable for X-ray diffraction studies for the adduct of $GaCl_3$ with $[P(p\text{-Anis})_3]$ and for the three adducts containing the tris(2,4,6-trimethoxyphenyl)phosphine (TMP) ligand. However, elemental analysis indicated that both moieties were present in a 1:1 ratio and solid-state ^{31}P NMR spectroscopy confirmed the Ga–P connectivity.

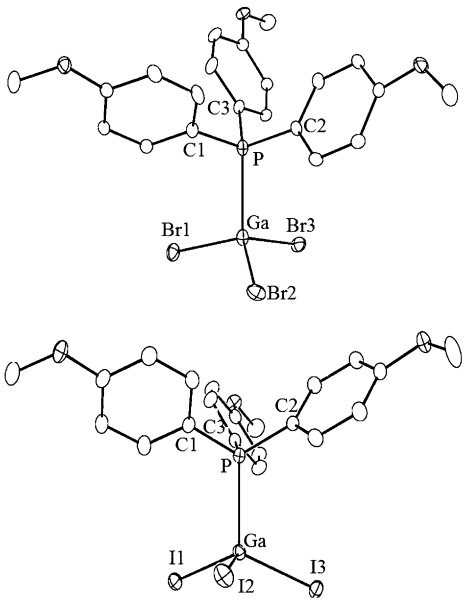

Figure 2. Molecular structures of $Br_3Ga[P(p\text{-Anis})_3]$ (top) and $I_3Ga[P(p\text{-Anis})_3]$ (bottom). For clarity, the hydrogen atoms are not shown.

$^{69/71}$Ga NMR of solid triarylphosphine gallium adducts: $^{69/71}$Ga NMR parameters determined from analyses of the spectra for the triarylphosphine gallium trihalide adducts investigated herein are listed in Table 1. See Figures S1–S4 in the Supporting Information, as well as those shown below, for examples of Ga NMR spectra. The signs for $C_{\mathrm{Q}}(^{69/71}\mathrm{Ga})$ reported in this section were determined from an analysis of the ^{31}P NMR spectra of MAS samples, or from the results of DFT calculations (see below).

Because $Br_3Ga[P(p\text{-Anis})_3]$ has a C_3 symmetry axis along the Ga–P bond, the Ga CS and EFG tensors are axially symmetric with the unique component of each tensor along the Ga–P bond; hence $\eta_{\mathrm{Q}}=0$ and $\kappa=\pm1$. The central transition peaks in the ^{71}Ga NMR spectra of MAS and stationary samples of $Br_3Ga[P(p\text{-Anis})_3]$, shown in Figure 3a and b, respectively, are broad and featureless; the broadening, attributed to the ^{71}Ga–$^{79/81}$Br residual dipolar interactions (^{79}Br: $I=3/2$, $\Xi=25.05\,\%$, NA $=50.69\,\%$; ^{81}Br: $I=3/2$, $\Xi=27.01\,\%$, NA $=49.31\,\%$),[20] leads to difficulties in determining the $C_{\mathrm{Q}}(^{71}\mathrm{Ga})$ value. The value for $C_{\mathrm{Q}}(^{71}\mathrm{Ga})$, $(+1.00\pm0.10)$ MHz, was obtained by analyzing the full ^{71}Ga NMR spectrum of a MAS sample, including

Table 1. Experimental $^{69/71}$Ga NMR parameters for $X_3Ga(PR_3)$ (X = Cl, Br, and I) adducts.

Gallium chemical shift tensor	δ_{iso} [ppm]	δ_{11} [ppm]	δ_{22} [ppm]	δ_{33} [ppm]	Ω [ppm]	κ
$Cl_3Ga(PPh_3)$	260.0±10.0	357.5±10.0	215.0±10.0	207.5±10.0	150.0±15.0	−0.90±0.10
$Br_3Ga(PPh_3)$	137.0±10.0	178.2±10.0	119.7±10.0	113.2±10.0	65.0±15.0	−0.80±0.10
$I_3Ga(PPh_3)$	−150.0±10.0	−30.0±10.0	−30.0±10.0	−390.0±10.0	360.0±15.0	1.00
$Cl_3Ga[P(p\text{-Anis})_3]$	256.0±3.0	342.0±3.0	220.0±3.0	207.0±3.0	135.0±4.0	−0.80±0.10
$Br_3Ga[P(p\text{-Anis})_3]$	138.0±7.0	164.7±7.0	124.7±7.0	124.7±7.0	40.0±10.0	−1.00
$I_3Ga[P(p\text{-Anis})_3]$	−135.0±7.0	−10.0±7.0	−31.0±7.0	−365.0±7.0	355.0±10.0	0.88±0.10
$Cl_3Ga(TMP)$	225.0±10.0	295.0±10.0	196.0±10.0	185.0±10.0	110.0±15.0	−0.80±0.10
$Br_3Ga(TMP)$	120.0±10.0	140.0±10.0	111.0±10.0	110.0±10.0	30.0±15.0	−0.90±0.10
$I_3Ga(TMP)$	−140.0±10.0	−7.0±10.0	−26.0±10.0	−387.0±10.0	380.0±15.0	0.90±0.10

Gallium quadrupolar coupling	$C_{\mathrm{Q}}(^{69}\mathrm{Ga})$ [MHz]	$C_{\mathrm{Q}}(^{71}\mathrm{Ga})$ [MHz]	η_{Q}	α [°]	β [°]	γ [°]
$Cl_3Ga(PPh_3)$	+3.00±0.20	+1.90±0.20	0.24±0.10	65±10	75±10	32±5
$Br_3Ga(PPh_3)$	±1.45±0.20	±0.90±0.20	0.10±0.10	80±10	50±10	30±10
$I_3Ga(PPh_3)$	+5.20±0.20	+3.30±0.20	0	0	0	0
$Cl_3Ga[P(p\text{-Anis})_3]$	+2.40±0.10	+1.50±0.10	0.16±0.10	80±10	85±5	5±10
$Br_3Ga[P(p\text{-Anis})_3]$	±1.60±0.10	±1.00±0.10	0	–	90	0
$I_3Ga[P(p\text{-Anis})_3]$	−6.80±0.20	−4.25±0.20	0.15±0.10	75±15	15±10	45±10
$Cl_3Ga(TMP)$	−14.30±0.40	−9.00±0.40	0.20±0.10	80±10	85±5	10±10
$Br_3Ga(TMP)$	−17.40±0.40	−11.00±0.40	0.24±0.10	30±10	85±5	10±10
$I_3Ga(TMP)$	−17.10±0.40	−10.70±0.40	0.35±0.10	60±10	10±10	50±10

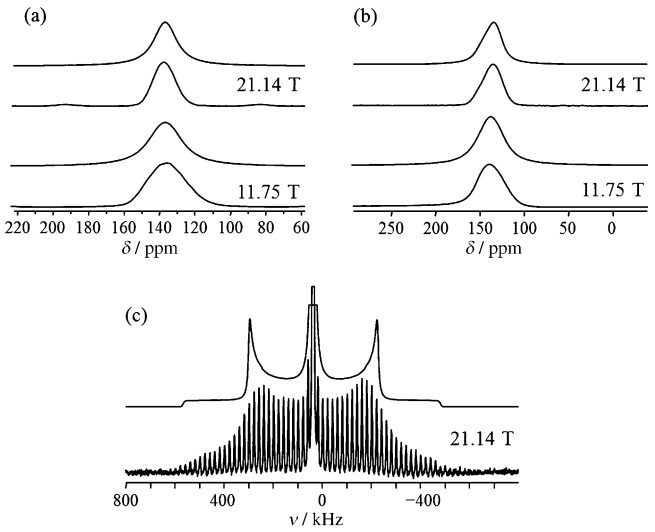

Figure 3. Experimental (lower traces) and calculated (upper traces) central transition in the ^{71}Ga NMR spectra of a) MAS and b) stationary powder samples of $Br_3Ga[P(p\text{-Anis})_3]$ acquired at 11.75 and 21.14 T. c) The NMR spectrum of the central and satellite transitions for a MAS sample (20.0 kHz) acquired at 21.14 T is shown in the lower trace with the simulated spectrum of a stationary sample shown in the upper trace; the peak arising from the central transition has been truncated in these images to emphasize the line shape of the spectrum arising from the satellite transitions.

the satellite transitions, as shown in Figure 3c. The small value for $C_Q(^{71}Ga)$ is consistent with the ^{31}P NMR spectra, that is, a negligible d value (see below). Powder line shapes arising from quadrupolar coupling cannot be discerned in these spectra, but the ^{71}Ga NMR spectrum of a stationary sample obtained at 21.14 T (Figure 3b) is asymmetric; this is attributed to anisotropic gallium magnetic shielding. This allowed the determination of the span of the gallium CS tensor, (40.0 ± 10.0) ppm, and of κ, −1.00. Thus, the unique components of the Ga CS and EFG tensors, δ_{11} and V_{ZZ}, respectively, are along the C_3 axis, in agreement with results of the DFT calculations.

The central transition peaks in the ^{71}Ga NMR spectra of both MAS and stationary samples (Figure S3 in the Supporting Information) of $Br_3Ga(PPh_3)$ are similar to those of $Br_3Ga[P(p\text{-Anis})_3]$, and thus were analyzed in the same manner. The broad and featureless peaks are also attributed to the ^{71}Ga–$^{79/81}$Br residual dipolar interactions. This adduct has an approximate C_3 symmetry axis about the Ga–P bond.[8] Analysis of the ^{71}Ga NMR spectra yielded similar values as for $Br_3Ga[P(p\text{-Anis})_3]$: $C_Q(^{71}Ga) = (\pm 0.90 \pm 0.20)$ MHz, $\eta_Q = (0.10 \pm 0.10)$, $\Omega = (65.0 \pm 15.0)$ ppm, and $\kappa = (-0.80 \pm 0.10)$. Hence, the EFG and CS tensors are almost axially symmetric with V_{ZZ} coincident with δ_{11}, both aligned approximately along the Ga–P bond.

Ga NMR spectra of the central transition of stationary samples of $I_3Ga(PPh_3)$ obtained at different magnetic-field strengths are shown in Figure 4. From the simulations, it is apparent that for ^{71}Ga at 7.05 T, the broadening arising from the magnetic shielding anisotropy is somewhat greater than that arising from the second-order nuclear quadrupolar interaction, the opposite of what is observed for the ^{69}Ga

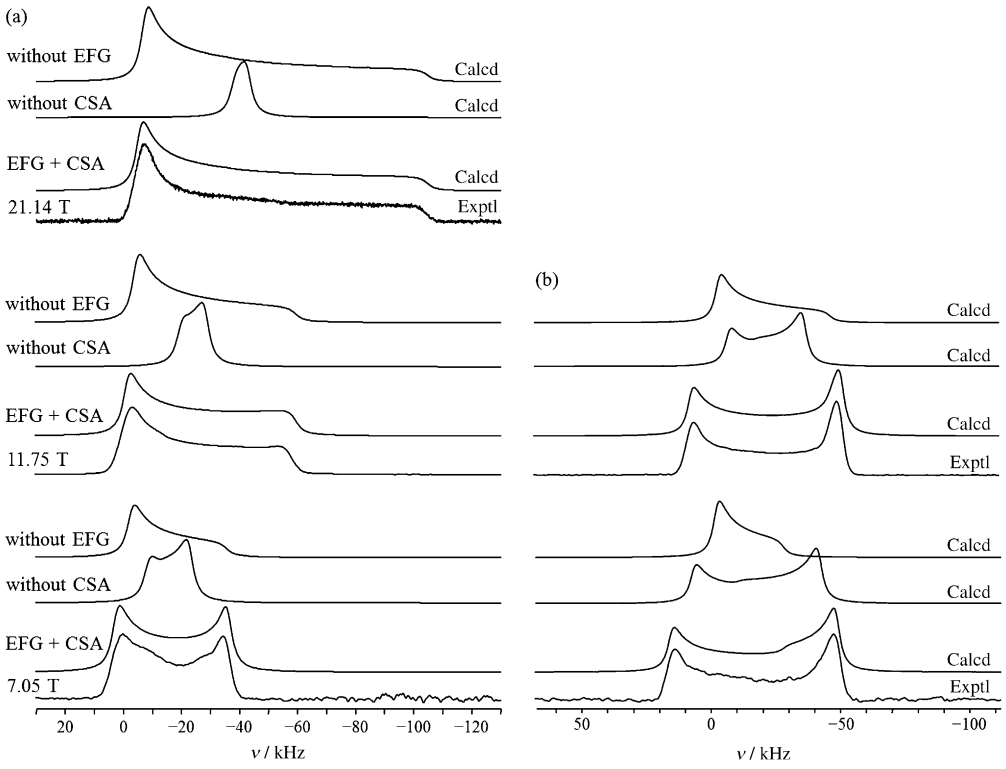

Figure 4. Experimental (lower traces) and calculated (upper traces) central transition in the a) ^{71}Ga and b) ^{69}Ga NMR spectra of stationary powder samples of $I_3Ga(PPh_3)$ acquired at 7.05, 11.75, and 21.14 T.

nuclei of this sample. For ^{69}Ga NMR spectra acquired at 11.75 T, the broadening arising from these two interactions is comparable. The contribution from the second-order quadrupolar interaction is negligible for ^{71}Ga NMR spectra acquired at 21.14 T. The differences discussed above arise because ^{69}Ga has a larger nuclear quadrupole moment and a smaller magnetic moment, combined with the fact that, in frequency units, the effects of the second-order quadrupolar interaction are inversely proportional to $\mathbf{B}_0$, whereas those of the magnetic shielding anisotropy are proportional to $\mathbf{B}_0$. The value of $C_Q(^{71}Ga)$ is $(+3.30\pm0.20)$ MHz and $\Omega=(360.0\pm15.0)$ ppm. Both the EFG and CS tensors at Ga in $I_3Ga(PPh_3)$ are axially symmetric, as expected from the presence of a C_3 symmetry axis, with $\eta_Q=0$ and $\kappa=1.00$. The skew indicates that δ_{33} is oriented along the Ga–P bond, in contrast to $Br_3Ga(PPh_3)$ and $Br_3Ga[P(p\text{-Anis})_3]$ in which δ_{11} is parallel or approximately parallel to the this bond. DFT calculations reproduce these orientations (see below).

The Ga NMR spectra of the central transition of stationary samples of $I_3Ga[P(p\text{-Anis})_3]$, obtained at three different magnetic-field strengths (Figure 5), are similar to those of $I_3Ga(PPh_3)$. The $C_Q(^{71}Ga)$ value is (-4.25 ± 0.20) MHz and $\Omega=(355.0\pm10.0)$ ppm; both the EFG and CS tensors at Ga in $I_3Ga[P(p\text{-Anis})_3]$ are close to axially symmetric ($\eta_Q=(0.15\pm0.10)$ and $\kappa=(0.88\pm0.10)$), as expected from the approximate C_3 symmetry axis that includes the gallium atom. The values of the asymmetry parameters indicate that δ_{33} and V_{ZZ} are oriented approximately along the Ga–P bond. $^{69/71}$Ga NMR spectra of $Cl_3Ga[P(p\text{-Anis})_3]$ are shown in Figure 6. The splitting in the ^{71}Ga NMR spectrum of a MAS sample obtained at 11.75 T is attributed to $^1J(^{71}Ga,^{31}P)$. The

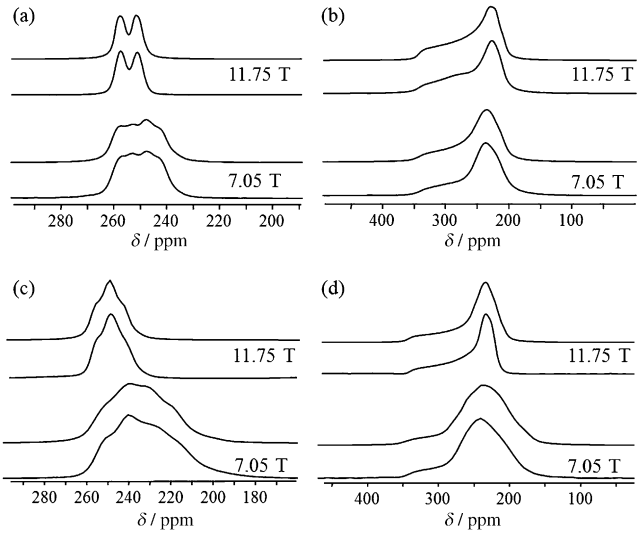

Figure 6. Experimental (lower traces) and calculated (upper traces) central transition in the ^{71}Ga NMR spectra of a) MAS and b) stationary powder samples of $Cl_3Ga[P(p\text{-Anis})_3]$ acquired at 7.05 and 11.75 T. The corresponding ^{69}Ga spectra of this compound are shown in c) (MAS) and d) (stationary).

$C_Q(^{71}Ga)$ value, $(+1.50\pm0.10)$ MHz, was determined from an analysis of the ^{71}Ga spectra of a MAS sample. The breadth of the peaks in the ^{71}Ga NMR spectra of a stationary sample, acquired at 7.05 and 11.75 T, plotted on the ppm scale in Figure 6b, are almost equal; this observation is a clear indication that magnetic shielding anisotropy dominates the ^{71}Ga NMR spectra of $Cl_3Ga[P(p\text{-Anis})_3]$. The span of the Ga CS tensor is (135.0 ± 4.0) ppm. The gallium η_Q and κ values, (0.16 ± 0.10) and (-0.80 ± 0.10), respectively,

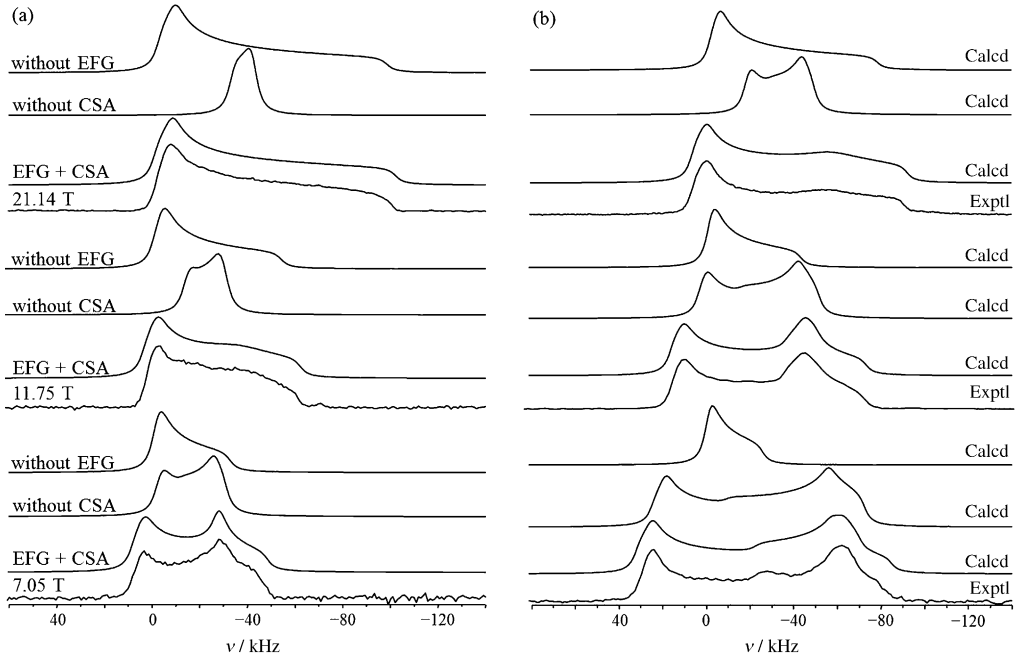

Figure 5. Experimental (lower traces) and calculated (upper traces) central transition in the a) ^{71}Ga and b) ^{69}Ga NMR spectra of stationary powder samples of $I_3Ga[P(p\text{-Anis})_3]$ acquired at 7.05, 11.75, and 21.14 T.

indicate that the EFG and CS tensors at Ga are close to axially symmetric with δ_{11} and V_{ZZ} both approximately in the direction of the Ga–P bond.

^{71}Ga NMR spectra of $Cl_3Ga(PPh_3)$ (Figure S4 in the Supporting Information) are similar to those of $Cl_3Ga[P(p\text{-Anis})_3]$. The $C_Q(^{71}Ga)$ value, $(+1.9\pm0.2)$ MHz, is slightly larger in magnitude than that for the latter, as is the span of the Ga CS tensor, (150 ± 15) ppm. The gallium η_Q and κ values, (0.24 ± 0.10) and (-0.9 ± 0.1), respectively, indicate that the EFG and CS tensors at Ga have a similar orientation to those for $Cl_3Ga[P(p\text{-Anis})_3]$, discussed above.

The Ga NMR spectra of the central transition of stationary samples of $X_3Ga(TMP)$ (X = Cl, Br and I), obtained at 11.75 T, are shown in Figure 7; the results of the analyses are summarized in Table 1. For a given adduct, the Ga NMR spectra have similar line shapes apart from the positions of the discontinuities in each spectrum, suggesting that they have similar Ga EFG tensors, but different Ga CS tensors.

The $|C_Q(^{71}Ga)|$ values for the gallium complexes investigated herein range from 0.9 to 11.0 MHz (Table 1). These are greatest for the adducts containing the bulky TMP ligand, but otherwise there is no clear relationship between the gallium C_Q value and the structures of the adducts. A comparison of adducts with the same triarylphosphine ligand indicates that the gallium nuclei are most and least shielded for X = I and Cl, respectively, as shown in Figure 8 and summarized in Table 1; this has been attributed to the spin-orbit effect of the halogen ligand.[27] Reported Ga chemical shift values for $X_3Ga(PPh_3)$ (X = Cl, Br, and I) in CD_2Cl_2 are 264, 152, and −151 ppm, respectively,[8] similar to the values and the trend obtained in this study. The same trend in indium chemical shifts has also been observed for the indium(III) trihalide triarylphosphine adducts.[18] The spans of the gallium magnetic shielding tensors for the adducts considered herein are largest for X = I (355 to 380 ppm) and smallest for X = Br (30 to 65 ppm).

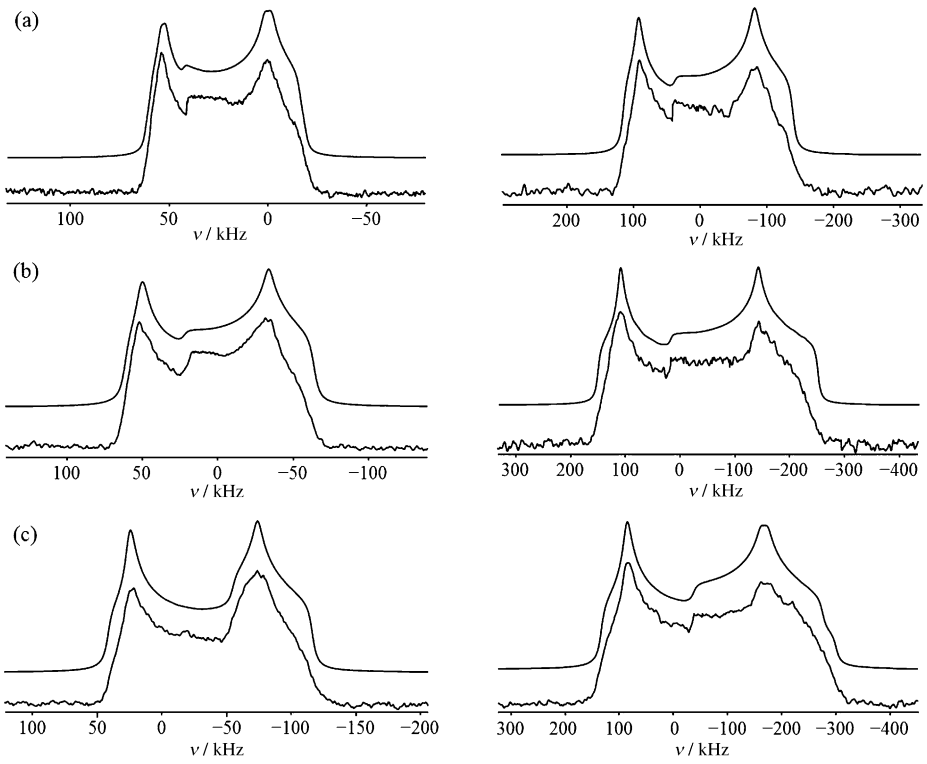

Figure 7. Experimental (lower traces) and calculated (upper traces) central transition in the ^{71}Ga (left) and ^{69}Ga NMR (right) spectra of stationary powder samples of a) $Cl_3Ga(TMP)$, b) $Br_3Ga(TMP)$, and c) $I_3Ga(TMP)$, acquired at 11.75 T.

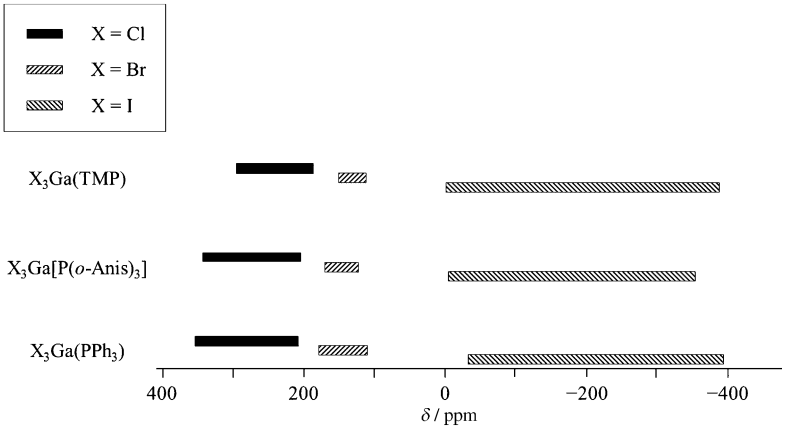

Figure 8. Spans of the CS tensors for $X_3Ga(TMP)$, $X_3Ga[P(p\text{-Anis})_3]$, and $X_3Ga(PPh_3)$.

Solid-state ^{31}P NMR spectroscopy: With a couple of exceptions, the $^1J(^{69/71}Ga,^{31}P)$ and $R_{eff}(^{69/71}Ga,^{31}P)$ values for the adducts considered herein are too small to be extracted from the Ga NMR spectra of stationary samples, but are available from ^{31}P NMR spectra acquired with MAS. Figures 9–11 provide examples of ^{31}P NMR spectra for several $X_3Ga(PR_3)$ adducts. From the relative magnetogyric ratios for

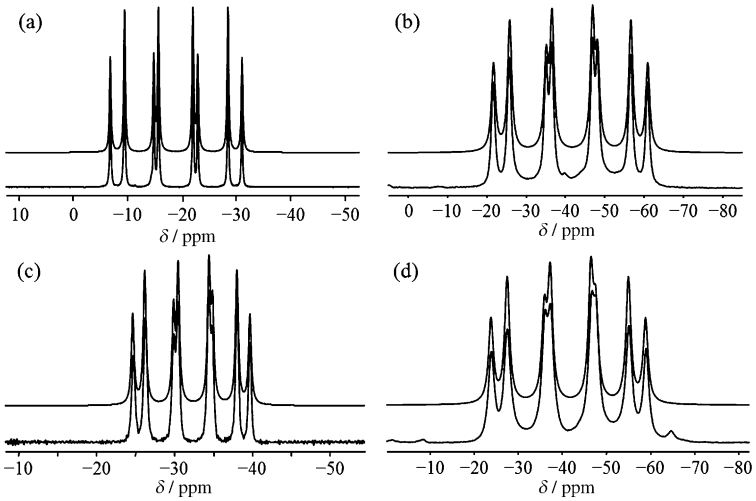

Figure 9. Experimental (lower traces) and calculated (upper traces) ^{31}P NMR spectra of MAS powder samples of a) $Cl_3Ga[P(p\text{-Anis})_3]$, b) $Cl_3Ga(TMP)$, c) $I_3Ga[P(p\text{-Anis})_3]$, and d) $Br_3Ga(TMP)$ acquired at 7.05 T.

^{69}Ga and ^{71}Ga, ^{31}P NMR spectra of MAS samples are expected to consist of two 1:1:1:1 quartets, arising from indirect spin–spin coupling to ^{69}Ga and ^{71}Ga, with an intensity ratio of 3:2, respectively, based on the natural abundances of the two gallium isotopes. Thus, one may expect to see eight peaks in the isotropic region of a ^{31}P NMR spectrum, as shown in Figure 9a. However, in most cases, not all the peaks are resolved as a consequence of the similar magnetogyric ratios for ^{69}Ga and ^{71}Ga, combined with relatively small $^1J(^{69/71}Ga,^{31}P)$ values and in some cases, broad peaks. Another important spin–spin parameter for the present work, $R_{eff}(^{69/71}Ga,^{31}P)$, may be estimated from ^{31}P NMR spectra of either stationary or MAS samples. The parameters derived from analyses of the ^{31}P NMR spectra are summarized in Table 2.

From the values for $R_{eff}(^{69/71}Ga,^{31}P)$ and $R_{dd}(^{69/71}Ga,^{31}P)$, the latter of which can be calculated from the Ga–P bond length, $\Delta J(^{69/71}Ga,^{31}P)$ may in some cases be estimated. In an earlier study, we showed that if the **J** and dipolar tensors are coincident with an exact or approximate C_3 symmetry axis incorporating the spin pair, then $d=(3C_QR_{eff})/(10\nu_S)$[18] (see also the Supporting Information). Table S3 in the Supporting Information summarizes the $2d$ values obtained in this study. With C_Q determined from the Ga NMR spectra and d determined from the ^{31}P NMR spectra of MAS samples, $R_{eff}(^{69/71}Ga,^{31}P)$ values can be determined from analyses of the ^{31}P NMR spectra. In our earlier work,[18] we also demonstrated that a 2.5% correction for librational effects[28] on measured values of R_{eff} or R_{DD} was sufficient for heavier atoms such as those in the Ga–P spin pairs considered herein. Hence, experimental dipolar couplings obtained from ^{31}P NMR spectra have been reduced by 2.5%.

Table 2. Experimental ^{31}P NMR parameters for $X_3Ga(PR_3)$ (X = Cl, Br, and I) adducts.

Phosphorus chemical shift tensor						
	δ_{iso} [ppm]	δ_{11} [ppm]	δ_{22} [ppm]	δ_{33} [ppm]	Ω [ppm]	κ
$Cl_3Ga(PPh_3)$	−8.1±1.0	5.6±1.0	−14.4±1.0	−15.4±1.0	21.0±2.0	−0.90±0.10
$Br_3Ga(PPh_3)$	−13.5±1.0	0.2±1.0	−19.8±1.0	−20.8±1.0	21.0±2.0	−0.90±0.10
$I_3Ga(PPh_3)$	−28.5±1.0	−15.2±1.0	−35.2±1.0	−35.2±1.0	20.0±2.0	−1.00
$Cl_3Ga[P(p\text{-Anis})_3]$	−18.9±1.0	5.8±1.0	−30.3±1.0	−32.2±1.0	38.0±2.0	−0.90±0.10
$Br_3Ga[P(p\text{-Anis})_3]$	−26.6±1.0	0.1±1.0	−39.9±1.0	−39.9±1.0	40.0±2.0	−1.00
$I_3Ga[P(p\text{-Anis})_3]$	−32.4±1.0	−13.9±1.0	−39.4±1.0	−43.9±1.0	30.0±2.0	−0.70±0.20
$Cl_3Ga(TMP)$	−41.4±1.0	−27.5±1.0	−47.3±1.0	−49.5±1.0	22.0±2.0	−0.80±0.10
$Br_3Ga(TMP)$	−41.7±1.0	−32.2±1.0	−45.7±1.0	−47.2±1.0	15.0±2.0	−0.80±0.10
$I_3Ga(TMP)$	−54.1±1.0	−47.8±1.0	−56.8±1.0	−57.8±1.0	10.0±2.0	−0.80±0.10

^{69}Ga–^{31}P spin–spin coupling				
	$^1J(^{69}Ga,^{31}P)$ [Hz]	$R_{eff}(^{69}Ga,^{31}P)$ [Hz][a]	$R_{dd}(^{69}Ga,^{31}P)$ [Hz]	$\Delta J(^{69}Ga,^{31}P)$ [Hz]
$Cl_3Ga(PPh_3)$	780±20	650±50	860±20	630±150
$Br_3Ga(PPh_3)$	620±20	550±50	840±20	870±150
$I_3Ga(PPh_3)$	300±20	550±50	810±20	780±150
$Cl_3Ga[P(p\text{-Anis})_3]$	770±20	750±50	860±20[b]	330±150
$Br_3Ga[P(p\text{-Anis})_3]$	640±20	580±50	730±20	450±150
$I_3Ga[P(p\text{-Anis})_3]$	480±20	700±50	830±20	390±150
$Cl_3Ga(TMP)$	1250±20	520±50	860±20[b]	1020±150
$Br_3Ga(TMP)$	1120±20	520±50	730±20[b]	630±150
$I_3Ga(TMP)$	850±20	500±50	810±20[b]	930±150

^{71}Ga–^{31}P spin–spin coupling				
	$^1J(^{71}Ga,^{31}P)$ [Hz]	$R_{eff}(^{71}Ga,^{31}P)$ [Hz][a]	$R_{dd}(^{71}Ga,^{31}P)$ [Hz]	$\Delta J(^{71}Ga,^{31}P)$ [Hz]
$Cl_3Ga(PPh_3)$	990±20	830±50	1090±20	780±150
$Br_3Ga(PPh_3)$	780±20	700±50	1060±20	1080±150
$I_3Ga(PPh_3)$	380±20	700±50	1030±20	990±150
$Cl_3Ga[P(p\text{-Anis})_3]$	980±20	950±50	1090±20[b]	420±150
$Br_3Ga[P(p\text{-Anis})_3]$	810±20	740±50	930±20	570±150
$I_3Ga[P(p\text{-Anis})_3]$	610±20	890±50	1050±20	480±150
$Cl_3Ga(TMP)$	1590±20	660±50	1090±20[b]	1290±150
$Br_3Ga(TMP)$	1420±20	660±50	930±20[b]	810±150
$I_3Ga(TMP)$	1080±20	630±50	1030±20[b]	1200±150

[a] $R_{eff}(^{69/71}Ga,^{31}P)$ values were obtained by correcting the observed values by −2.5%. [b] Estimated (see text).

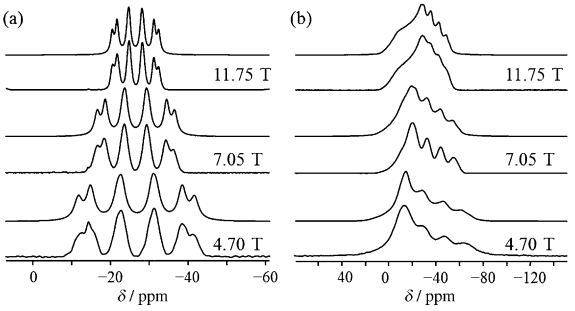

Figure 10. Experimental (lower traces) and calculated (upper traces) ^{31}P NMR spectra of a) MAS and b) stationary powder samples of $Br_3Ga[P(p\text{-Anis})_3]$ acquired at 4.70, 7.05, and 11.75 T.

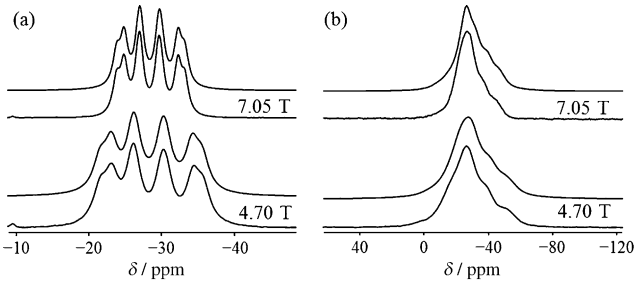

Figure 11. Experimental (lower traces) and calculated (upper traces) ^{31}P NMR spectra of a) MAS and b) stationary powder samples of $I_3Ga(PPh_3)$ acquired at 4.70 and 7.05 T.

A detailed discussion of the analysis of the data for the $Br_3Ga[P(p\text{-Anis})_3]$ adduct (Figure 10) is presented as an example. The equally spaced peaks in this spectrum indicate that d is negligible and therefore that the gallium C_Q values are very small, precluding an experimental assignment of a sign for this interaction; these were thus assigned from the DFT calculations (see below). Values of (810 ± 20) and (740 ± 50) Hz for $^1J(^{71}Ga,^{31}P)$ and $R_{eff}(^{71}Ga,^{31}P)$, respectively, were obtained from analyses of the spectra of MAS and stationary samples (Figure 10). From the known Ga–P bond length, 2.500 Å, an uncorrected value of (950 ± 20) Hz was obtained for R_{DD}; this is reduced to (930 ± 20) Hz after applying the correction for librational motion discussed above. Furthermore, since this adduct contains a C_3 symmetry axis along its Ga–P bond, ΔJ can be calculated by using $\Delta J = 3(R_{DD}-R_{eff})$, allowing an estimate of $\Delta J(^{71}Ga,^{31}P)$, which depends on the sign of R_{eff}. Values for ΔJ of $(+570\pm150)$ or $(+5010\pm150)$ Hz are thus obtained. An analysis of ^{31}P NMR spectra of stationary samples showed that $^1J(^{71}Ga,^{31}P)$ and $R_{eff}(^{71}Ga,^{31}P)$ have the same sign. Since one-bond spin–spin coupling constants in analogous compounds are positive,[18,29,30] $^1J(^{71}Ga,^{31}P)$ and R_{eff} are expected to be positive[31,32] and thus, the smaller of the two possible values for ΔJ is more probable. Hence, $\Delta J(^{71}Ga,^{31}P)$ and $^1J(^{71}Ga,^{31}P)$ are both positive and have similar magnitudes. This conclusion is supported by calculations (see below).

The $I_3Ga(PPh_3)$ adduct also has a C_3 axis along the Ga–P bond.[9] Analyses of the ^{31}P NMR spectra of MAS and stationary samples (Figure 11) are similar to those of $Br_3Ga[P(p\text{-Anis})_3]$. However, in this case, the $2d$ value obtained at 4.70 T, +20 Hz, is apparent; the $C_Q(^{71}Ga)$ value is thus relatively large and had to be included in the analysis, which indicates that the sign of $C_Q(^{71}Ga)$ is positive, as for $C_Q(^{69}Ga)$. These results agree with those obtained from DFT calculations (see below). A comparable analysis was performed for $Cl_3Ga(PPh_3)$ and $I_3Ga[P(p\text{-Anis})_3]$.

The analysis outlined above assumes that the **J** and dipolar tensors are coincident and axially symmetric. Significant differences between R_{eff} and R_{DD} must be a consequence of $\Delta J(^{69/71}Ga,^{31}P)$, and since the analysis yields comparable values of $\Delta J(^{69/71}Ga,^{31}P)$ for closely related adducts, the deviation from axial symmetry is not thought to be sufficient to significantly affect the values obtained. As discussed above, these analyses assumed that the signs of $^1J(^{69/71}Ga,^{31}P)$ for these adducts are positive; DFT calculations (see below) support this assumption.

Although Ga–P bond lengths are unavailable for several adducts considered herein, examination of the data for similar adducts in References [8] and [9] and in this study (Table S2 in the Supporting Information) indicate that there is little variation in the Ga–P bond lengths for a given halide. Since R_{eff} values, determined for all adducts, are of comparable magnitudes (Table 2), $\Delta J(^{69/71}Ga,^{31}P)$ is expected to be significant in all cases considered herein. Hence, values for $\Delta J(^{69/71}Ga,^{31}P)$ have been estimated based on the smallest corrected value of R_{DD} (and thus the smallest value for $\Delta J(^{69/71}Ga,^{31}P)$) predicted from the Ga–P bond lengths for a given halide; these are summarized in Table 2.

Previously, the nature of the bond between a spin–spin coupled pair has been explained based on the assumption that the coupling is dominated by the Fermi-contact mechanism.[33] Although a similar conclusion appears to be consistent with the results of DFT calculations discussed below, it is important to consider that the Fermi contact term does not contribute to ΔJ;[23,24] hence the observation of $\Delta J(^{69/71}Ga,^{31}P)$ for these adducts indicates that mechanisms other than the Fermi-contact term also make significant contributions to $^1\mathbf{J}(^{69/71}Ga,^{31}P)$.[24]

To summarize, $^1J(^{69/71}Ga,^{31}P)$ and $\Delta J(^{69/71}Ga,^{31}P)$ values, as well as their signs, have been determined for all $X_3Ga(PR_3)$ adducts investigated herein. These are of comparable magnitude and are positive. Signs for $C_Q(^{69/71}Ga)$ have also been determined for those adducts that have C_3 symmetry and for which the $^{69/71}Ga$–^{31}P residual dipolar coupling was observable.

Solution-phase ^{31}P NMR spectroscopy: $^{31}P\{^1H\}$ NMR spectra of $Br_3Ga[P(p\text{-Anis})_3]$ dissolved in deuterated chloroform and acquired at various temperatures are shown in Figure S9 of the Supporting Information. At 323 K, two overlapping multiplets due to $^1J(^{69}Ga,^{31}P)$ and $^1J(^{71}Ga,^{31}P)$ are apparent. The value of $^1J(^{71}Ga,^{31}P)$ is approximately 810 Hz (estimated error 10%) in agreement with the value obtained in the solid state, (810 ± 20) Hz (see Table 2). At temperatures less than 300 K, the $^{69/71}Ga$–^{31}P spin–spin coupling splitting pat-

terns collapse as a result of rapid $^{69/71}$Ga spin-lattice relaxation.[34] At 213 K, the $^{69/71}$Ga nuclei are essentially self-decoupled from the ^{31}P nuclei (i.e., $\{2\pi[J(^{69/71}\text{Ga},^{31}\text{P})][T_1(^{69/71}\text{Ga})]\}^2 \ll 0.1$).[34,35] Similar results were obtained for $I_3Ga[P(p\text{-Anis})_3]$ (see Figure S10 in the Supporting Information) and for $I_3Ga(PPh_3)$.

In some cases, we observed broadening of the overlapping 1:1:1:1 multiplets with increasing temperature, which we attribute to ligand exchange at higher temperatures. Likewise, Cheng et al. found that it was necessary to cool samples below room temperature to decrease the rate of ligand exchange sufficiently to observe $^1J(^{69/71}\text{Ga},^{31}\text{P})$ for $X_3Ga(PPh_3)$ (X = Cl and Br) dissolved in CH_2Cl_2.[8] Clearly, an interplay of the magnitude of the $^{69/71}$Ga nuclear quadrupolar coupling constants, rotational correlation times, rate of ligand exchange, and the magnitude of $^1J(^{69/71}\text{Ga}, ^{31}\text{P})$ will dictate exactly what line shape one will observe in solution as a function of temperature. To obtain accurate values of $^1J(^{69/71}\text{Ga},^{31}\text{P})$ from ^{31}P NMR spectra acquired in solution, it would be necessary to carry out detailed line-shape analyses as outlined in the review by Mlynárik,[34] but we were able to obtain reasonable estimates of these values for the $X_3Ga(PR_3)$ adducts (see Table 3). As shown in Tables 2 and 3, the same trend is observed for solid samples and for samples in solution. $^1J(^{69/71}\text{Ga},^{31}\text{P})$ values decrease slightly as X changes from Cl to Br and more dramatically as X changes from Cl or Br to I.

Table 3. Solution-phase ^{31}P NMR parameters for $X_3Ga(PR_3)$ (X = Cl, Br, and I) adducts.

	$\delta_{iso}(^{31}\text{P})$ [ppm]	$^1J(^{71}\text{Ga},^{31}\text{P})$ [Hz]	T [K]
$Cl_3Ga(PPh_3)$	−5.5 ± 0.2	721 ± 10	183[a]
	−5.6 ± 0.2	793 ± 10	193
$Br_3Ga(PPh_3)$	−10.7 ± 0.2	693 ± 10	273[a]
	−10.3 ± 0.2	696 ± 10	193
$I_3Ga(PPh_3)$	−29.7 ± 0.2	466 ± 10	273[a]
	−28.7 ± 0.2	470 ± 10	253
$Cl_3Ga[P(p\text{-Anis})_3]$	−18.8 ± 0.2	970 ± 10	RT
$Br_3Ga[P(p\text{-Anis})_3]$	−24.8 ± 0.2	810 ± 10	323
$I_3Ga[P(p\text{-Anis})_3]$	−31.4 ± 0.2	535 ± 10	333
$Cl_3Ga(TMP)$	−41.7 ± 0.2	[b]	193
$Br_3Ga(TMP)$	−45.8 ± 0.2	[b]	233
$I_3Ga(TMP)$	−52.8 ± 0.2	[b]	193

[a] Reference [8]. [b] Only one broad peak was observed and the $^1J(^{71}\text{Ga},^{31}\text{P})$ values could not be resolved.

These results demonstrate that, because of the competing mechanisms occurring for samples in solution, it generally is easier to characterize indirect spin–spin coupling constants involving quadrupolar nuclei in the solid state.

DFT calculations—Comparison with experiment: Calculated Ga NMR parameters are summarized in Table 4. A comparison of experimental and calculated $C_Q(^{69/71}\text{Ga})$ values (Tables 1 and 4) shows that the DFT calculations do not reproduce experimental trends, but they do correctly predict that these values are small (e.g., for the diatomic gallium(I) halides, $C_Q(^{69}\text{Ga})$ ranges from −106.6 for GaF to −81.1 MHz for GaI, an order of magnitude larger than the values for the gallium(III) adducts investigated herein).[36] In addition, the calculated sign for $C_Q(^{69/71}\text{Ga})$ is reproduced for the seven adducts for which it is known from experiments. Furthermore, the calculated relative orientations of the gallium EFG and shielding tensors, given by the Euler angles α, β, and γ, are in qualitative agreement with experimental values. For example, consider the two complexes that have an exact C_3 axis along the Ga–P bond, $Br_3Ga[P(p\text{-Anis})_3]$ and $I_3Ga(PPh_3)$. Despite the small gallium and phosphorus spans, calculations correctly predict that the unique components of the EFG and CS tensors are V_{ZZ} and δ_{11} for the former and V_{ZZ} and δ_{33} for the latter.

Converting calculated shielding into chemical shifts requires the establishment of an absolute shielding scale for the nucleus of interest.[37] Since no such scale has been established for gallium, the gallium shielding constant for $[Ga(H_2O)_6]^{3+}$ was calculated to approximate that of the accepted gallium chemical shift reference, $Ga(NO_3)_3$ (1.0 M).[20] This value, $\sigma = 1814$ ppm, was set to $\delta_{iso}(Ga) = 0$ ppm and thus the calculated chemical shift values in Table 4 were ob-

Table 4. Calculated $^{69/71}$Ga NMR parameters for $X_3Ga(PR_3)$ and model $X_3Ga(PMe_3)$ (X = Cl, Br, and I) adducts.[a]

Gallium chemical shift tensors

	δ_{iso} [ppm]	δ_{11} [ppm]	δ_{22} [ppm]	δ_{33} [ppm]	Ω [ppm]	κ
$Cl_3Ga(PPh_3)$	344	473	291	270	203	−0.79
$Br_3Ga(PPh_3)$	171	205	156	153	52	−0.89
$I_3Ga(PPh_3)$	−212	−30	−30	−575	545	1.00
$Cl_3Ga[P(p\text{-Anis})_3]$	344	468	295	268	200	−0.73
$Br_3Ga[P(p\text{-Anis})_3]$	130	152	119	119	33	−1.00
$I_3Ga[P(p\text{-Anis})_3]$	−189	−8	−34	−525	517	0.90
$Cl_3Ga(TMP)$	313	409	278	253	156	−0.69
$Br_3Ga(TMP)$	101	140	86	78	62	−0.75
$I_3Ga(TMP)$	−190	31	−87	−515	547	0.57
$Cl_3Ga(PMe_3)$	354	469	304	288	180	−0.83
$Br_3Ga(PMe_3)$	135	144	138	122	22	0.44
$I_3Ga(PMe_3)$	−178	37	−15	−555	591	0.82

Gallium quadrupolar coupling

	$C_Q(^{69}\text{Ga})$ [MHz]	$C_Q(^{71}\text{Ga})$ [MHz]	η_Q	α [°]	β [°]	γ [°]
$Cl_3Ga(PPh_3)$	+8.3	+5.2	0.17	73	88	17
$Br_3Ga(PPh_3)$	+4.6	+2.8	0.39	80	84	50
$I_3Ga(PPh_3)$	+5.6	+3.5	0.00	0	0	0
$Cl_3Ga[P(p\text{-Anis})_3]$	+5.9	+3.7	0.47	83	88	10
$Br_3Ga[P(p\text{-Anis})_3]$	+11.0	+6.9	0.00	90	90	0
$I_3Ga[P(p\text{-Anis})_3]$	−3.3	−2.1	0.52	85	37	47
$Cl_3Ga(TMP)$	−6.8	−4.3	0.36	79	77	11
$Br_3Ga(TMP)$	−11.4	−7.1	0.04	27	87	0
$I_3Ga(TMP)$	−3.2	−2.0	0.32	72	46	30
$Cl_3Ga(PMe_3)$	+6.6	+4.1	0.11	84	73	6
$Br_3Ga(PMe_3)$	+12.7	+8.0	0.01	17	89	18
$I_3Ga(PMe_3)$	−4.2	−2.6	0.17	86	30	30

[a] Chemical shifts converted from shielding values according to $\delta_{iso}(Ga) = 1814 - \sigma_{iso}(Ga)$ (see text).

tained from calculated magnetic shielding values by using the relationship $\delta(Ga)_{calcd} = 1814 - \sigma(Ga)_{calcd}$.

Plots of experimental versus calculated $\delta_{iso}(Ga)$, κ, and Ω values are shown in Figure 12; these indicate that the calculated chemical shift parameters are qualitatively in agreement with the corresponding experimental values. For the three series of complexes studied, $X_3Ga(PPh_3)$, $X_3Ga[P(p\text{-}Anis)_3]$, and $X_3Ga(TMP)$, δ_{iso} is greatest for X = Cl and least for X = I, in agreement with experiments; this is illustrated in Figure 13. Likewise, calculated and experimental Ω values are in agreement (compare Figure 13 with Figure 8). To investigate the origin of the increased gallium shielding as the atomic number of the halogen atom increases, the so-called normal halogen effect (NHE), the diamagnetic (σ_{dia}), paramagnetic (σ_{para}), and spin-orbital ($\sigma_{spin-orbit}$) contributions to the gallium isotropic magnetic shielding constants were calculated (see Table S4 in the Supporting Information). The value of σ_{dia} is virtually independent of the halogen, and σ_{para} tends to decrease slightly as X changes from Cl to I; however, it is clearly $\sigma_{spin-orbit}$ that is responsible for the observed NHE, with contributions from $\sigma_{spin-orbit}$ to the isotropic shielding of gallium of approximately 160, 370, and 745 ppm for X = Cl, Br, and I, respectively. Significantly, although both σ_{para} and $\sigma_{spin-orbit}$ are significantly anisotropic, there is little variation in the anisotropy of the former, regardless of the halogen atom. In contrast, the anisotropy in $\sigma_{spin-orbit}$ varies from less than 30 ppm for the trichloro adducts to more than 700 ppm for the triiodo adducts (Table S4 in the Supporting Information). Hence, $\sigma_{spin-orbit}$ is also responsible for the large spans in the gallium chemical shift tensors for the triiodo adducts in comparison with those for the tribromides and trichlorides.

In contrast to the Ga^{III} adducts, Ga^{I} monohalides exhibit an inverse halogen dependence (IHD).[38] Likewise, we recently reported an NHE for a series of In^{III} trihalides in contrast to the IHD found for some In^{I} monohalides.[18] In both the gallium and indium series of compounds, a large paramagnetic term (largest for X = I and smallest for X = Cl) is mainly responsible for the IHD of the isotropic chemical shifts for the monohalides (see Table S5 in the Supporting Information).

Calculated $^1J(^{69/71}Ga,^{31}P)$ and $\Delta J(^{69/71}Ga,^{31}P)$ values for the $X_3Ga(PR_3)$ adducts are listed in Table 5. The former are generally smaller than the observed values; nevertheless the experimental trend that $^1J(^{69/71}Ga,^{31}P)$ is greatest for X = Cl and smallest for X = I is reproduced by the calculations. Calculated

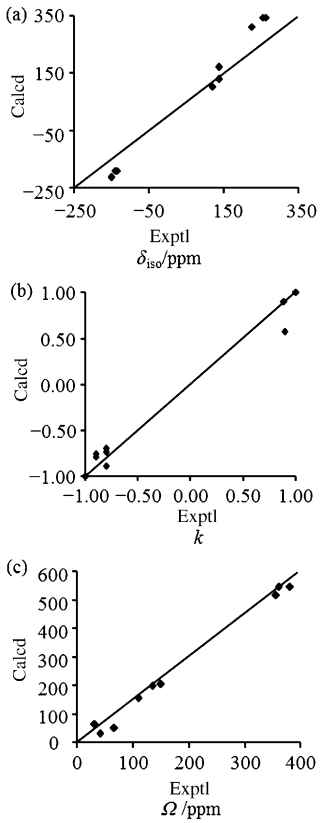

Figure 12. Experimental versus calculated gallium CS tensor values a) δ_{iso}, b) κ, and c) Ω for the gallium trihalide triarylphosphine adducts $X_3Ga(PR_3)$. The solid line indicates perfect agreement between experimental and calculated values. The standard deviations ($s = [\Sigma(calcd-exptl)^2/(n-1)]^{1/2}$ in which n is the number of data points) are 64 ppm, 0.14, and 111 ppm for δ_{iso}, κ, and Ω, respectively.

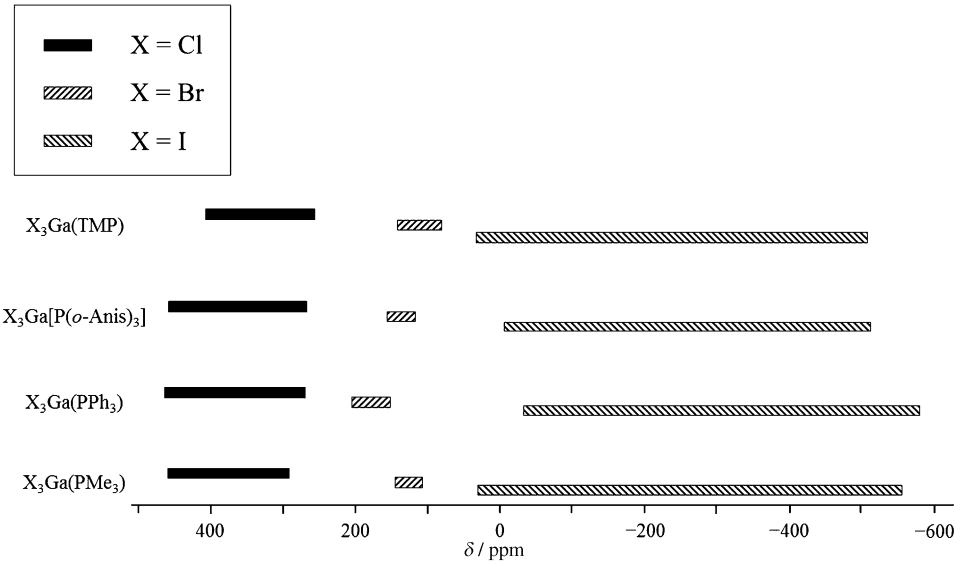

Figure 13. Calculated spans of the CS tensors for $X_3Ga(TMP)$, $X_3Ga[P(p\text{-}Anis)_3]$, $X_3Ga(PPh_3)$, and $X_3Ga(PMe_3)$.

Table 5. Calculated $^{1}J(^{69/71}Ga,^{31}P)$ and $\Delta J(^{69/71}Ga,^{31}P)$ for $X_3Ga(PR_3)$ and model $X_3Ga(PMe_3)$ (X = Cl, Br, and I) adducts.

	$^{1}J(^{69}Ga,^{31}P)$ [Hz]	$^{1}J(^{71}Ga,^{31}P)$ [Hz]	$\Delta J(^{69}Ga,^{31}P)$ [Hz]	$\Delta J(^{71}Ga,^{31}P)$ [Hz]
$Cl_3Ga(PPh_3)$	+344	+437	+511	+650
$Br_3Ga(PPh_3)$	+211	+268	+484	+615
$I_3Ga(PPh_3)$	+6	+8	+391	+496
$Cl_3Ga[P(p\text{-Anis})_3]$	+404	+513	+536	+682
$Br_3Ga[P(p\text{-Anis})_3]$	+218	+277	+480	+609
$I_3Ga[P(p\text{-Anis})_3]$	+89	+114	+448	+569
$Cl_3Ga(TMP)$	+469	+596	+555	+705
$Br_3Ga(TMP)$	+254	+322	+471	+598
$Cl_3Ga(PMe_3)$	+388	+492	+549	+697
$Br_3Ga(PMe_3)$	+181	+229	+469	+596
$I_3Ga(PMe_3)$	+52	+66	+466	+592

values of $\Delta J(^{71}Ga,^{31}P)$ are positive and range from approximately 500 to 700 Hz, whereas the experimental values range for (420 ± 150) to (1290 ± 150) Hz. Although the errors in the experimental values are large, it is clear that the anisotropies in the indirect Ga–P spin–spin coupling tensors are on the same order of magnitude as the isotropic values. The calculated contribution of the Fermi-contact mechanism to $^{1}J(^{69/71}Ga,^{31}P)_{iso}$ (not shown) for the model adducts is approximately 99%. The calculations indicate that the nonzero $\Delta J(^{69/71}Ga,^{31}P)$ values result from the spin-dipolar Fermi-contact (SD × FC) cross term. Thus, both the Fermi-contact and spin-dipolar Fermi-contact mechanisms make important contributions to the $\mathbf{J}(^{69/71}Ga,^{31}P)$ tensors in these adducts. A similar effect was noted for the $\mathbf{J}(^{113/115}In,^{31}P)$ tensors of indium(III) trihalide phosphine adducts.[18]

Conclusion

The results of an investigation of several triarylphosphine gallium trihalide adducts, $X_3Ga(PR_3)$ (X = Cl, Br, or I; PR_3 = triarylphosphine ligand) by using solid-state $^{69/71}Ga$ and ^{31}P NMR spectroscopy and single-crystal X-ray diffraction has been presented. The experimental $C_Q(^{71}Ga)$ values for these adducts range from $(+3.3 \pm 0.2)$ to (-11.0 ± 0.4) MHz; the signs of $C_Q(^{69/71}Ga)$ for some adducts with an exact or approximate C_3 axis were determined from analyses of the ^{31}P NMR spectra. The $^{69/71}Ga$ nuclear quadrupolar coupling constants reported herein are small compared with others that we have previously measured in our lab. The relatively small EFGs at the gallium nuclei in these compounds are in agreement with the predictions of Bancroft and coworkers.[39]

Trends observed in this study are similar to those observed for the related In–phosphine adducts.[18] In particular, the gallium nuclei are most shielded for X = I and least shielded for X = Cl, that is, the normal halogen effect. The anisotropic gallium magnetic shielding is measurable for all adducts, with spans as large as (380 ± 15) ppm. Similar to observations for the In–phosphine adducts, the spans are greatest for the adducts with X = I; for $^{69/71}Ga$ spectra acquired at 21.14 T, the contribution from this interaction to the NMR line shape of the central transition is of the same magnitude or greater than that from $C_Q(^{69/71}Ga)$. Values for $^{1}J(^{69/71}Ga,^{31}P)$ were determined for all adducts investigated herein. In addition, $\Delta J(^{69/71}Ga,^{31}P)$ values and their signs are reported; these were derived from known or estimated values for R_{DD}. As for the ^{115}In–^{31}P **J** tensors,[18] the $^{1}J(^{69/71}Ga,^{31}P)$ and $\Delta J(^{69/71}Ga,^{31}P)$ values are comparable in magnitude and positive.

Solution-phase ^{31}P NMR spectroscopic results indicate that the gallium T_1 relaxation times for $I_3Ga(PPh_3)$, $Br_3Ga[P(p\text{-Anis})_3]$, and $I_3Ga[P(p\text{-Anis})_3]$ are very short at lower temperatures, whereas those for $Cl_3Ga(PPh_3)$, $Br_3Ga(PPh_3)$, and $Cl_3Ga[P(p\text{-Anis})_3]$ do not change significantly in comparison to changes in the Ga–phosphine exchange rates. The differences between the solution-phase ^{31}P NMR spectra for these adducts at different temperatures are attributed to a competition between variations in the $^{69/71}Ga$ T_1 values and in the Ga-phosphine exchange rates. The ^{31}P NMR parameters, $^{1}J(^{71}Ga,^{31}P)$ and $\delta_{iso}(^{31}P)$, measured in solution, are generally in agreement with those obtained from solid-state NMR spectroscopy.

The experimental results have been complemented by relativistic DFT calculations. These calculations qualitatively reproduce the available experimental $^{69/71}Ga$ EFG and CS tensors, including their relative orientations, and they also reproduce the normal halogen effect observed between the isotropic gallium magnetic shielding and the halogen ligands; calculations confirm that this effect is due to the spin-orbital effect of the halogen ligand. Although calculated values of $^{1}J(^{69/71}Ga,^{31}P)$ and $\Delta J(^{69/71}Ga,^{31}P)$ are generally lower than the experimental values, calculations undertaken for the $X_3Ga(PR_3)$ adducts confirm that $^{1}J(^{69/71}Ga,^{31}P)$ and $\Delta J(^{69/71}Ga,^{31}P)$ are comparable in magnitude with positive signs. Calculations indicate that both the Fermi-contact and spin-dipolar Fermi-contact mechanisms are important factors when considering the **J** tensor between coupled gallium and phosphorus nuclei.

We have provided herein an interpretation of solid-state $^{69/71}Ga$ NMR spectra for some gallium–phosphine complexes. The conclusions reached in this study are comparable to those reached in an earlier study of indium–phosphine complexes:[18] one may not ignore the effects of gallium magnetic shielding anisotropy, particularly for spectra acquired at high magnetic-field strengths; relativistic DFT calculations are helpful in the analysis of $^{69/71}Ga$ NMR spectra; and NMR investigations of spin-$^1/_2$ nuclei, such as ^{31}P, coupled to gallium complement the $^{69/71}Ga$ NMR studies.

Experimental and Computational Details

Sample preparation: Gallium(III) chloride ($GaCl_3$), gallium(III) bromide ($GaBr_3$), gallium(III) iodide (GaI_3), triphenylphosphine (PPh_3), tris-*para*-methoxyphenylphosphine ($P(p\text{-Anis})_3$), and tris(2,4,6-trimethoxyphenyl)-phosphine (TMP) were purchased from either Aldrich or Strem and used as received. Owing to the ease of hydrolysis of the anhydrous halides and oxidation of the phosphine ligands, all operations were carried out in a

dry glovebox filled with argon. See the Supporting Information for more details of these syntheses and of the syntheses of the $X_3Ga(TMP)$ compounds, X = Cl, Br, and I, which have not previously been reported.

Single-crystal X-ray diffraction: Single crystals of $Br_3Ga[P(p\text{-Anis})_3]$ and $I_3Ga[P(p\text{-Anis})_3]$ suitable for X-ray diffraction were grown by very slow evaporation of solutions of these complexes in a 1:1 mixture of ethyl acetate and dichloromethane. Suitable crystals were mounted on glass fibers by means of paratone-N oil, and data were collected at 193 K by using graphite-monochromated $Mo_{K\alpha}$ radiation (0.71073 Å) on a Bruker PLATFORM/SMART 1000 CCD diffractometer. The structures were solved by direct methods using SHELXS-97[40] and refined using full-matrix least-squares on F^2 (SHELXL-97).[40] All nonhydrogen atoms in the compounds were refined with anisotropic displacement parameters. Selected crystal data and structure refinement details for $Br_3Ga[P(p\text{-Anis})_3]$ and $I_3Ga[P(p\text{-Anis})_3]$ are listed in Tables S1 and S2 in the Supporting Information. CCDC-896761 ($Br_3Ga[P(p\text{-Anis})_3]$) and CCDC-896762 ($I_3Ga[P(p\text{-Anis})_3]$) contain the supplementary crystallographic data for this paper. These data can be obtained free of charge from The Cambridge Crystallographic Data Centre via www.ccdc.cam.ac.uk/data_request/cif.

NMR spectroscopy: Solution-phase $^{31}P\{^1H\}$ NMR spectra were acquired at 161.902 MHz on a three-channel Varian Inova 400 MHz (^1H) spectrometer by using a pulsed field gradient direct detection broadband switchable probe. Reported temperatures are based on a calibration curve for that probe. The low-temperature portion of the calibration curve was constructed by using a standard methanol sample from Varian. The solvent used for the $X_3Ga(PPh_3)$ and $X_3Ga(TMP)$ adducts was CD_2Cl_2 whereas $CDCl_3$ was used for the $X_3Ga[P(p\text{-Anis})_3]$ complexes.

Solid-state ^{31}P NMR spectra of MAS and stationary samples were acquired on a Chemagnetics CMX Infinity 200 ($B_0 = 4.70$ T), as well as Bruker Avance 300 and 500 NMR spectrometers by using the combination of standard cross-polarization (CP) with proton TPPM decoupling.[41] Samples were packed in 4 mm o.d. rotors. Proton 90° pulse widths of 4.0 μs, contact times of 5 to 10 ms, and pulse delays of 4 to 60 s were used to acquire most ^{31}P NMR spectra. ^{31}P chemical shifts were referenced with respect to 85% aqueous phosphoric acid by setting the isotropic peak of an external solid ammonium dihydrogen phosphate sample to 0.81 ppm.[42] Spectra of MAS samples were acquired at ambient temperature with a spinning frequency of 8.0 to 15.0 kHz.

$^{69/71}$Ga NMR spectra of MAS and stationary samples were acquired on Bruker Avance 300 ($B_0 = 7.05$ T), 500 ($B_0 = 11.75$ T) and Avance II 900 MHz ($B_0 = 21.14$ T) NMR spectrometers by using Bruker 4 mm MAS probes. Spectra of MAS samples were acquired at ambient temperature with a spinning frequency of 12.5 to 20.0 kHz. A $\pi/2$–τ_1–$\pi/2$–τ_2–ACQ echo sequence was used to acquire all Ga NMR spectra, with pulse lengths ($\tau_{p(sel)}$) that selectively excited the central transition, $\tau_{(sel)} = \tau_{(non\text{-}sel)}/(S+^1/_2) = \tau_{(non\text{-}sel)}/2$ for $^{69/71}$Ga.[43] Proton TPPM decoupling[41] was used to acquire all spectra. Each step of the Ga NMR spectra acquired at 7.05 or 11.75 T is the sum of 4096 to 72000 scans. Ga NMR chemical shifts were referenced with respect to an external solution of $Ga(NO_3)_3$ (1.0 M).[20] The relaxation delay was 0.5 s.

^{311}P and $^{69/71}$Ga NMR parameters were determined by visual comparison of experimental NMR spectra with those simulated by using the WSolids software package.[44] This software includes the quadrupolar interaction to second-order perturbation theory for simulations of $^{69/71}$Ga NMR spectra, and includes spin–spin interactions with these nuclei for simulations of ^{31}P NMR spectra of MAS samples.

Quantum chemical calculations: DFT calculations of gallium EFG[45] and CS[46] tensors, as well as $^1J(^{69/71}Ga,^{31}P)$ and $\Delta J(^{69/71}Ga,^{31}P)$ values,[47] were performed by using the Amsterdam Density Functional (ADF) program.[48] Geometries used for calculations for the $Cl_3Ga(PPh_3)$,[8] $Br_3Ga(PPh_3)$,[8] $I_3Ga(PPh_3)$,[9] $Br_3Ga[P(p\text{-Anis})_3]$, and $I_3Ga[P(p\text{-Anis})_3]$ adducts were those obtained from X-ray diffraction, except for the C–H bond lengths, which were fixed at 1.08 Å. Because single-crystal structure data for $Cl_3Ga[P(p\text{-Anis})_3]$, $Cl_3Ga(TMP)$, $Br_3Ga(TMP)$, and $I_3Ga(TMP)$ were unavailable, the geometries for $Cl_3Ga(PPh_3)$, $Br_3Ga[P(p\text{-Anis})_3]$, and $I_3Ga[P(p\text{-Anis})_3]$ were used, with the H atoms replaced by a methoxy group where needed (e.g., the *para*-H atom of PPh_3 was replaced with a methoxy group to model the P(*p*-Anis) ligand). To investigate the effects of the halides on the gallium magnetic shielding, CS tensors for model $X_3Ga(PMe_3)$ (X = Cl, Br, or I) adducts were also calculated. See the Supporting Information for more details.

Acknowledgements

We thank Victor Terskikh and Shane Pawsey for helpful comments and for acquiring some NMR spectra at 21.14 T. We are very grateful to Jason Clyburne, Gang Wu, Neil Burford, Klaus Eichele, Chris Kirby, Mike Lumsden, and Kenneth Wright for early contributions to this project. Access to the 900 MHz NMR spectrometer was provided by the National Ultrahigh-Field NMR Facility for Solids (Ottawa, Canada), funded by the Canada Foundation for Innovation, the Ontario Innovation Trust, Recherche Québec, the National Research Council of Canada, and Bruker BioSpin and managed by the University of Ottawa (www.nmr900.ca). R.G.C. and R.E.W. thank the Natural Sciences and Engineering Research Council of Canada (NSERC) for financial support through the Discovery Grant Program and for a Major Resources Support grant. R.E.W. also thanks the Canada Research Chairs program for research support.

[1] J. L. Gay-Lussac, J. L. Thénard, *Mem. Phys. Chim. Soc. d'Arcueil* **1809**, *2*, 210, as cited in: V. Jonas, G. Frenking, *J. Chem. Soc. Chem. Commun.* **1994**, 1489–1490.

[2] See, for example: a) S. J. Geier, T. M. Gilbert, D. W. Stephan, *Inorg. Chem.* **2011**, *50*, 336–344; b) E. I. Davydova, T. N. Sevastianova, A. V. Suvorov, A. Y. Timoshkin, *Coord. Chem. Rev.* **2010**, *254*, 2031–2077; c) F. Dornhaus, S. Scholz, I. Sänger, M. Bolte, M. Wagner, H.-W. Lerner, *Z. Anorg. Allg. Chem.* **2009**, *635*, 2263–2272; d) T. J. Clark, C. A. Jaska, A. Turak, A. J. Lough, Z.-H. Lu, I. Manners, *Inorg. Chem.* **2007**, *46*, 7394–7402.

[3] a) A. Staubitz, A. P. M. Robertson, M. E. Sloan, I. Manners, *Chem. Rev.* **2010**, *110*, 4023–4078; b) C. W. Hamilton, R. T. Baker, A. Staubitz, I. Manners, *Chem. Soc. Rev.* **2009**, *38*, 279–293; c) J. M. Brunel, B. Faure, M. Maffei, *Coord. Chem. Rev.* **1998**, *178–180*, 665–698.

[4] See, for example: a) A. Kuczkowski, S. Schulz, M. Nieger, *Eur. J. Inorg. Chem.* **2001**, 2605–2611; b) A. Kuczkowski, S. Schulz, M. Nieger, P. R. Schreiner, *Organometallics* **2002**, *21*, 1408–1419; c) R. L. Wells, R. A. Baldwin, P. S. White, W. T. Pennington, A. L. Rheingold, G. P. A. Yap, *Organometallics* **1996**, *15*, 91–97; d) R. L. Wells, S. R. Aubuchon, S. S. Kher, M. S. Lube, P. S. White, *Chem. Mater.* **1995**, *7*, 793–800.

[5] a) P. O'Brien, N. L. Pickett in *Comprehensive Coordination Chemistry II, Vol. 9* (Eds.: J. A. McCleverty, T. J. Meyer), Elsevier, Oxford, **2003**, pp. 1005–1063; b) I. R. Grant in *Chemistry of Aluminium, Gallium, Indium and Thallium* (Ed.: A. J. Downs), Blackie, Glasgow, **1993**, Chapter 5, pp. 292–321.

[6] a) A. J. Carty, *Can. J. Chem.* **1967**, *45*, 345–351; b) A. J. Carty, *Can. J. Chem.* **1967**, *45*, 3187–3192; c) A. J. Carty, T. Hinsperger, P. M. Boorman, *Can. J. Chem.* **1970**, *48*, 1959–1970.

[7] For recent reviews, see a) S. Arai, N. Nishiyama, T. Maruyama, T. Okumura, *IEEE J. Sel. Top. Quantum Electron.* **2011**, *17*, 1381–1389; b) S. L. Pyshkin, J. M. Ballato in *Advances and Applications in Electroceramics, Vol. 226* (Eds.: K. M. Nair, Q. Jia, S. Priya), Wiley, Hoboken, **2011**, Chapter 18, pp. 77–90; c) D. J. Friedman, J. M. Olson, S. Kurtz in *Handbook of Photovoltaic Science and Engineering*, 2nd ed. (Eds.: A. Luque, S. Hegedus), Wiley, Chichester, **2011**, pp. 314–337.

[8] F. Cheng, H. L. Codgbrook, A. L. Hector, W. Levason, G. Reid, M. Webster, W. Zhang, *Polyhedron* **2007**, *26*, 4147–4155.

[9] M. A. Brown, J. A. Castro, D. G. Tuck, *Can. J. Chem.* **1997**, *75*, 333–341.

[10] a) F. Cheng, A. L. Hector, W. Levason, G. Reid, M. Webster, W. Zhang, *Inorg. Chem.* **2007**, *46*, 7215–7223; b) J. F. Janik, R. A. Baldwin, R. L. Wells, W. T. Pennington, G. L. Schimek, A. L. Rheingold, L. M. Liable-Sands, *Organometallics* **1996**, *15*, 5385–5390; c) L.-J.

Baker, L. A. Kloo, C. E. F. Rickard, M. J. Taylor, *J. Organomet. Chem.* **1997**, *545–546*, 249–255; d) L.-J. Baker, C. E. F. Rickard, M. J. Taylor, *J. Organomet. Chem.* **1994**, *464*, C4–C6; e) M. Sigl, A. Schier, H. Schmidbaur, *Eur. J. Inorg. Chem.* **1998**, 203–210; f) J. C. Carter, G. Jugie, R. Enjalbert, J. Galy, *Inorg. Chem.* **1978**, *17*, 1248–1254.

[11] a) T. Vosegaard, I. P. Byriel, L. Binet, D. Massiot, H. J. Jakobsen, *J. Am. Chem. Soc.* **1998**, *120*, 8184–8188; b) T. Vosegaard, D. Massiot, *Chem. Phys. Lett.* **2007**, *437*, 120–125; c) L. A. O'Dell, S. L. P. Savin, A. V. Chadwick, M. E. Smith, *Appl. Magn. Reson.* **2007**, *32*, 527–546; d) J. T. Ash, P. J. Grandinetti, *Magn. Reson. Chem.* **2006**, *44*, 823–831; e) D. Massiot, I. Farnan, N. Gautier, D. Trumeau, A. Trokiner, J. P. Coutures, *Solid State Nucl. Magn. Reson.* **1995**, *4*, 241–248.

[12] a) J. P. Yesinowski, *Phys. Status Solidi C* **2005**, *2*, 2399–2402; b) W.-S. Jung, O. H. Han, S.-A. Chae, *Mater. Chem. Phys.* **2006**, *100*, 199–202; c) A. P. Purdy, J. P. Yesinowski, A. T. Hanbicki, *Phys. Status Solidi C* **2005**, *2*, 2437–2440; d) J. P. Yesinowski, *J. Magn. Reson.* **2006**, *180*, 147–161; e) J. P. Yesinowski, A. P. Purdy, *J. Am. Chem. Soc.* **2004**, *126*, 9166–9167.

[13] a) D. Franke, H. Eckert, R. B. Kaner, R. E. Treece, *Anal. Chim. Acta* **1993**, *283*, 987–995; b) D. P. Tunstall, A. Rogerson, *J. Phys. C: Solid State Phys.* **1979**, *12*, 3105–3120.

[14] a) J. M. Kikkawa, D. D. Awschalom, *Science* **2000**, *287*, 473–476; b) T. Ota, N. Kumada, G. Yusa, S. Miyashita, Y. Hirayama, *Phys. Status Solidi C* **2007**, *4*, 1759–1762; c) J. Takeuchi, H. Nakamura, H. Yamada, E. Kita, A. Tasaki, T. Erata, *Solid State Nucl. Magn. Reson.* **1997**, *8*, 123–128; d) L. D. Potter, Y. Wu, *J. Magn. Reson. Ser. A* **1995**, *116*, 107–112; e) O. H. Han, H. K. C. Timken, E. Oldfield, *J. Chem. Phys.* **1988**, *89*, 6046–6052.

[15] For recent examples, see a) A. T. Durant, K. J. D. MacKenzie, H. Maekawa, *Dalton Trans.* **2011**, *40*, 4865–4870; b) F. Blanc, D. S. Middlemiss, Z. Gan, C. P. Grey, *J. Am. Chem. Soc.* **2011**, *133*, 17662–17672; c) H. B. Yahia, L. van Wüllen, S. Balamurugan, U. Ch. Rodewald, H. Eckert, R. Pöttgen, *Z. Naturforsch. B* **2011**, *66*, 14–20.

[16] J. F. Hinton, R. W. Briggs in *NMR and the Periodic Table* (Eds.: R. K. Harris, B. E. Mann), Academic Press, London, **1978**, Chapter 9, p. 285–286.

[17] T. Vosegaard, D. Massiot, N. Gautier, H. J. Jakobsen, *Inorg. Chem.* **1997**, *36*, 2446–2450.

[18] F. Chen, G. Ma, G. M. Bernard, R. G. Cavell, R. McDonald, M. J. Ferguson, R. E. Wasylishen, *J. Am. Chem. Soc.* **2010**, *132*, 5479–5493.

[19] F. Chen, G. Ma, R. G. Cavell, V. V. Terskikh, R. E. Wasylishen, *Chem. Commun.* **2008**, 5933–5935.

[20] R. K. Harris, E. D. Becker, S. M. Cabral de Menezes, R. Goodfellow, P. Granger, *Pure Appl. Chem.* **2001**, *73*, 1795–1818.

[21] J. Mason, *Solid State Nucl. Magn. Reson.* **1993**, *2*, 285–288.

[22] For several current articles, see a) P. P. Man in *NMR of Quadrupolar Nuclei in Solid Materials* (Eds.: R. E. Wasylishen, S. E. Ashbrook, S. Wimperis), Wiley, Chichester, **2012**, Chapter 1, pp. 3–16; b) A. J. Vega in *NMR of Quadrupolar Nuclei in Solid Materials* (Eds.: R. E. Wasylishen, S. E. Ashbrook, S. Wimperis), Wiley, Chichester, **2012**, Chapter 2, pp. 17–44; c) S. E. Ashbrook, S. Wimperis in *NMR of Quadrupolar Nuclei in Solid Materials* (Eds.: R. E. Wasylishen, S. E. Ashbrook, S. Wimperis), Wiley, Chichester, **2012**, Chapter 3, pp. 45–61; d) D. L. Bryce, R. E. Wasylishen in *NMR of Quadrupolar Nuclei in Solid Materials* (Eds.: R. E. Wasylishen, S. E. Ashbrook, S. Wimperis), Wiley, Chichester, **2012**, Chapter 4, pp. 63–74; e) D. C. Apperley, R. K. Harris, P. Hodgkinson, *Solid State NMR: Basic Principles and Practice*, Momentum Press, New York, **2012**, Chapter 6, pp. 141–175; see also, f) J. P. Amoureux, C. Fernandez, P. Granger in *Multinuclear Magnetic Resonance in Liquids and Solids—Chemical Applications* (Eds.: P. Granger, R. K. Harris), Kluwer Academic, Dordrecht, **1990**, pp. 409–424; g) A. Abragam, *Principles of Nuclear Magnetism*, Clarendon Press, Oxford, **1961**, Chapter VII, pp. 216–263.

[23] A. D. Buckingham, I. Love, *J. Magn. Reson.* **1970**, *2*, 338–351.

[24] a) R. E. Wasylishen in *Encyclopedia of Nuclear Magnetic Resonance, Vol. 3* (Eds.: D. M. Grant, R. K. Harris), Wiley, Chichester, **1996**, pp. 1685–1695; b) R. E. Wasylishen in *Encyclopedia of Nuclear Magnetic Resonance, Vol. 9* (Eds.: D. M. Grant, R. K. Harris), Wiley, Chichester, **2002**, pp. 274–282, and references therein.

[25] a) R. K. Harris, A. C. Olivieri, *Prog. Nucl. Magn. Reson. Spectrosc.* **1992**, *24*, 435–456, and references cited therein; b) R. K. Harris, A. C. Olivieri in *Encyclopedia of Nuclear Magnetic Resonance, Vol. 9* (Eds.: D. M. Grant, R. K. Harris), Wiley, Chichester, **2002**, pp. 141–150; c) P. Grondona, A. C. Olivieri, *Concepts Magn. Reson.* **1993**, *5*, 319–339.

[26] D. L. VanderHart, H. S. Gutowsky, T. C. Farrar, *J. Am. Chem. Soc.* **1967**, *89*, 5056–5057.

[27] a) M. Sugimoto, M. Kanayama, H. Nakatsuji, *J. Phys. Chem.* **1993**, *97*, 5868–5874; b) H. Takashima, M. Hada, H. Nakatsuji, *Chem. Phys. Lett.* **1995**, *235*, 13–16.

[28] J. Manz, *J. Am. Chem. Soc.* **1980**, *102*, 1801–1806.

[29] a) H. Nöth, B. Wrackmeyer in *NMR Basic Principles and Progress, Vol 14, Nuclear Magnetic Resonance Spectroscopy of Boron Compounds* (Eds.: P. Diehl, E. Fluck, R. Kosfeld), **1978**, Springer, Berlin, pp. 104–105; b) H. C. E. McFarlane, W. McFarlane, D. S. Rycroft, *J. Chem. Soc. Faraday Trans. 2* **1972**, *68*, 1300–1305.

[30] a) R. W. Rudolph, C. W. Schultz, *J. Am. Chem. Soc.* **1971**, *93*, 6821–6822; b) A. H. Cowley, M. C. Damasco, *J. Am. Chem. Soc.* **1971**, *93*, 6815–6821.

[31] a) C. J. Jameson in *Multinuclear NMR* (Ed.: J. Mason), Plenum Press, New York, **1987**, Chapter 4, pp. 89–131; b) C. J. Jameson in *Phosphorus-31 NMR Spectroscopy in Stereochemical Analysis, Organic Compounds and Metal Complexes* (Eds.: J. G. Verkade, L. D. Quin) VCH, Deerfield Beach, **1987**, Chapter 6, pp. 205–230.

[32] R. E. Wasylishen, K. C. Wright, K. Eichele, T. S. Cameron, *Inorg. Chem.* **1994**, *33*, 407–408.

[33] F. Chen, S.-W. Oh, R. E. Wasylishen, *Can. J. Chem.* **2009**, *87*, 1090–1101.

[34] V. Mlynárik, *Prog. Nucl. Magn. Reson. Spectrosc.* **1986**, *18*, 277–305.

[35] J. Bacon, R. J. Gillespie, J. W. Quail, *Can. J. Chem.* **1963**, *41*, 3063–3069.

[36] V. B. Singh, *J. Phys. Chem. Ref. Data* **2005**, *34*, 23–37.

[37] C. J. Jameson in *Encyclopedia of Nuclear Magnetic Resonance, Vol 2* (Eds.: D. M. Grant, R. K. Harris), Wiley, Chichester, **1996**, pp. 1273–1281.

[38] M. Gee, R. E. Wasylishen in *ACS Symposium Series, No. 732, Modeling NMR Chemical Shifts, Gaining Insights into Structure and Environment* (Eds.: J. C. Facelli, A. C. de Dios), American Chemical Society, Washington, **1999**, Chapter 19, pp. 259–276.

[39] a) G. M. Bancroft, R. H. Piatt, *Adv. Inorg. Chem. Radiochem.* **1972**, *15*, 59–258; b) G. M. Bancroft, T. K. Sham, *J. Magn. Reson.* **1977**, *25*, 83–90.

[40] G. M. Sheldrick, *Acta Crystallogr. Sect. A* **2008**, *64*, 112–122.

[41] A. E. Bennett, C. M. Rienstra, M. Auger, K. V. Lakshmi, R. G. Griffin, *J. Chem. Phys.* **1995**, *103*, 6951–6958.

[42] K. Eichele, R. E. Wasylishen, *J. Phys. Chem.* **1994**, *98*, 3108–3113.

[43] P. R. Bodart, J.-P. Amoureux, Y. Dumazy, R. Lefort, *Mol. Phys.* **2000**, *98*, 1545–1551.

[44] K. Eichele, R. E. Wasylishen, *WSOLIDS, Version 2.0.18*, University of Alberta, Edmonton, **2000**.

[45] E. van Lenthe, E. J. Baerends, *J. Chem. Phys.* **2000**, *112*, 8279–8292.

[46] G. Schreckenbach, T. Ziegler, *J. Phys. Chem.* **1995**, *99*, 606–611.

[47] a) J. Autschbach, T. Ziegler, *J. Chem. Phys.* **2000**, *113*, 9410–9418; b) J. Autschbach, T. Ziegler, *J. Chem. Phys.* **2000**, *113*, 936–947.

[48] a) *ADF, 2006.01*, Theoretical Chemistry, Vrije Universiteit, Amsterdam, **2006**, http://www.scm.com; b) G. te Velde, F. M. Bickelhaupt, E. J. Baerends, C. Fonseca Guerra, S. J. A. van Gisbergen, J. G. Snijders, T. Ziegler, *J. Comput. Chem.* **2001**, *22*, 931–967; c) C. Fonseca Guerra, J. G. Snijders, G. te Velde, E. J. Baerends, *Theor. Chem. Acc.* **1998**, *99*, 391–403.

Received: August 19, 2012
Published online: January 10, 2013

